Annexin A2 binding to endosomes and functions in endosomal transport are regulated by tyrosine 23 phosphorylation

Morel, Etienne ; Gruenberg, Jean

Abstract: The phospholipid-binding annexin A2 (AnxA2) is known to play a role in the regulation of membrane and actin dynamics, in particular in the endocytic pathway. The protein is present on early endosomes, where it regulates membrane traffic, including the biogenesis of multivesicular transport intermediates destined for late endosomes. AnxA2 membrane association depends on the protein N terminus and membrane cholesterol but does not involve the AnxA2 ligand p11/S100A10. However, the precise mechanisms that control AnxA2 membrane association and function are not clear. In the present study, we have investigated the role of AnxA2 N-terminal phosphorylation in controlling association to endosomal membranes and functions. We found that endosomal AnxA2 was partially tyrosine-phosphorylated and that mutation of Tyr-23 to Ala (AnxA2Y23A), but not of Ser-25 to Ala, impaired AnxA2 endosome association. We then found that the AnxA2Y23A mutant was unable to bind endosomes in vivo, whereas a phospho-mimicking AnxA2 mutant (Y23D) showed efficient endosome binding capacity. Similarly, we found that AnxA2Y23D interacted more efficiently with liposomes in vitro when compared with AnxA2Y23A. To investigate the role of Tyr-23 in vivo, AnxA2 was knocked down with small interfering RNAs, and then cells were recomplemented with RNA interference-resistant forms of the protein. Using this strategy, we could show that AnxA2Y23D, but not AnxA2Y23A, could restore early-to-late endosome transport after AnxA2 depletion. We conclude that phosphorylation of Tyr-23 is essential for proper endosomal association and function of AnxA2, perhaps because it stabilizes membrane-associated protein via a conformational change.

DOI: https://doi.org/10.1074/jbc.M806499200

Membrane Transport Structure Function and Biogenesis:

Annexin A2 binding to endosomes and functions in endosomal transport are regulated by tyrosine 23 phosphorylation

Etienne Morel and Jean Gruenberg

J. Biol. Chem. published online November 5, 2008

Access the most updated version of this article at doi: 10.1074/jbc.M806499200

JBC Papers in Press. Published on November 5, 2008 as Manuscript M806499200
The latest version is at http://www.jbc.org/cgi/doi/10.1074/jbc.M806499200

ANNEXIN A2 BINDING TO ENDOSOMES AND FUNCTIONS IN ENDOSOMAL TRANSPORT ARE REGULATED BY TYROSINE 23 PHOSPHORYLATION*

Etienne Morel and Jean Gruenberg
Department of Biochemistry, University of Geneva, Sciences II,
Quai E. Ansermet, 30, Geneva-4, Switzerland.
Running head: tyrosine phosphorylation regulates annexin A2 endosome binding
Address correspondence to: Jean Gruenberg, Department of Biochemistry, University of Geneva, 30 quai E. Ansermet, 1211 Geneva 4, Switzerland:
Tel: +41-22-379.6464; Fax: +41-22-379.6470; e-mail: jean.gruenberg@biochem.unige.ch.

The phospholipid-binding annexin A2 (AnxA2) is known to play a role in the regulation of membrane and actin dynamics, in particular in the endocytic pathway. The protein is present on early endosomes, where it regulates membrane traffic, including the biogenesis of multivesicular transport intermediates destined for late endosomes. AnxA2 membrane association depends on the protein N-terminus and membrane cholesterol, but does not involve the AnxA2 ligand p11/S100A10. However, the precise mechanisms that control AnxA2 membrane association and function are not clear. In the present study, we have investigated the role of AnxA2 N-terminal phosphorylation in controlling association to endosomal membranes and functions. We found that endosomal AnxA2 was partially tyrosine-phosphorylated, and that mutation of Tyr23 to Ala (AnxA2Y23A), but not of Ser25 to Ala, impaired AnxA2 endosome association. We then found that the AnxA2Y23A mutant was unable to bind endosomes in vivo, while a phospho-mimicking AnxA2 mutant (Y23D) showed efficient endosome binding capacity. Similarly, we found that AnxA2Y23D interacted more efficiently with liposomes in vitro, when compared to AnxA2Y23A. To investigate the role of Tyr23 in vivo, AnxA2 was knocked down with siRNAs and then cells were re-complemented with RNAi-resistant forms of the protein. Using this strategy, we could show that AnxA2Y23D, but not AnxA2Y23A, could restore early-to-late endosome transport after AnxA2 depletion. We conclude that phosphorylation of Tyr23 is essential for proper endosomal association and function of AnxA2, perhaps because it stabilizes membrane-associated protein via a conformational change.

Annexin family proteins, which can bind membranes via negatively charged phospholipids and Ca^{2+} ions (1), are considered as scaffolding proteins that can participate and/or regulate membrane dynamics and organization (2,3). Annexin A2 (AnxA2), a well-characterized member of this family, is composed of a non-folded and hyper-variable N-Terminal domain and of a very conserved C-terminal domain, which bears the common characteristics of annexins, including Ca^{2+} binding site and annexins repeats. The N-terminus of AnxA2 binds p11/S100A10, the light-chain of anxA2, leading to formation of the $(AnxA2)_2$-$(p11)_2$ heterotetramer (4). AnxA2 N-terminus also bears two phosphorylation sites, on Tyr23 and Ser25, which are presumably targets of Src kinase and protein kinase C, respectively (5-7), but their precise(s) role(s) are still under debate. The phosphorylation of Ser25 may play a role in vesicles/granules aggregation (8,9). The phosphorylation of Tyr23 by Src kinase was proposed to act either as a targeting signal for the plasma membrane together with p11 (10,11) or as a negative signal for $(AnxA2)_2$-$(p11)_2$ heterotetramer formation or stabilization (12). The presence of AnxA2 at the plasma membrane may also facilitate tyrosine phosphorylation (13). Tyrosine phosphorylation has also been proposed to regulate actin AnxA2-related functions (14), notably in polarized epithelial cells (15). Finally, AnxA2 has been identified as a Lyn kinase target after oxidative stress and phosphorylation was proposed to induce AnxA2 relocalization to the endoplasmic reticulum (16).

In fibroblastic cells or non-endothelial cells, AnxA2 is present at the plasma membrane, in the cytosol and also on early endosomes (2,17). Knockdown experiments by RNAi have shown that AnxA2 is involved in

early endosome membrane dynamics along the recycling (18) and degradation pathways (19,20). In particular, AnxA2 was shown to be required for the biogenesis of multivesicular transport intermediates destined for late endosomes (19,20). In contrast to other annexins, the endosomal association of AnxA2 does not depend on Ca^{2+} (17,21), or p11 binding and heterotetramer formation (20), but on membrane cholesterol (19,22,23). AnxA2 shows a non-random distribution on early endosomal membranes, presumably corresponding to cholesterol-AnxA2 platforms or domains (22). In addition, AnxA2 membrane association also requires the N-terminus of the protein (19,21,23,24), which contains the Tyr23 and Ser25 phosphorylation sites.

In the present article, we have analyzed the putative role of the phosphorylation of the AnxA2 N-terminal part in its association to early endosomes and in its endosomal functions. We show that purified endosomal anxA2 is tyrosine-phosphorylated and, by the use of phosphorylation mutants, we demonstrate that the phosphorylation of tyrosine 23 is required for a proper AnxA2 targeting to early endosome. Moreover, using a siRNA phenotype rescuing, we demonstrate that the AnxA2 function in the endosomal transport is controlled by tyrosine phosphorylation. We conclude that AnxA2 endosomal binding properties as well as the AnxA2 endosomal function are directly linked to tyrosine, but not serine, phosphorylation.

EXPERIMENTAL PROCEDURES

Cells, antibodies and reagents - Baby Hamster kidney cells (BHK21) and HeLa cells were grown as previously described (19,25). The monoclonal antibody against Rab5 was a gift from R. Jahn (Göttingen, Germany), monoclonal antibodies against AnxA2 (HH7 and H28) and p11 (H21) were gifts from V. Gerke (Münster, Germany). Rabbit polyclonal antibodies against EEA1 (early endosomal antigen 1) and Lamp1 (lysosomal associated membrane protein 1) were from Alexis Biochemical and Affinity Bioreagents respectively. The monoclonal antibody against GFP was from Roche Diagnostics, against transferrin receptor from Zymed Laboratories, and against phosphotyrosine from Transduction Laboratories (PY20) and Upstate (4G10). The monoclonal antibody against actin and polyclonal antibody against anti-phosphoserine were from Abcam. The rabbit polyclonal antibody against Rab7 was described (26,27). Peroxidase-conjugated secondary antibodies were from BioRad and Cy2, Cy3 and Cy5-conjugated fluorescent secondary antibodies were from Jackson Immunoresearch. The 10 kDa fluorescent fluid phase marker rhodamin-dextran was from Molecular Probes. F-actin was labeled with Allexa fluor 486nm coupled phalloidin from Invitrogen. All lipids and Latrunculin B were from Sigma.

Plasmids, recombinant proteins and RNAi - cDNA plasmid coding for human AnxA2A65E^{GFP} was a gift from V. Gerke (Münster, Germany). This plasmid is referred as AnxA2*wt*^{GFP} in the paper. From this cDNA, we cloned several mutants of anxA2^{GFP} by mutagenesis: anxA2*dmt*^{GFP} (anxA2$Y_{23}AS_{25}A^{GFP}$), in which Tyr23 and Ser25 were replaced by alanine, anxA2$Y_{23}A^{GFP}$, anxA2$Y_{23}D^{GFP}$ and anxA2$S_{25}A^{GFP}$. Similar recombinant AnxA2 constructions were obtained by cloning these cDNAs in pGEX-5X-1 expressing vector (Clontech) and GST-protein was produced in BL21 bacteria strain. The GST tag was removed by Factor Xa cleavage and benzamidine treatment (Amersham). The quality of recombinant protein was checked by SDS-PAGE and Coomassie staining. For mock-treated controls (ctrl) in RNAi experiments, we used VSV-G (Vesicular Stomatisis Virus, protein G) siRNA. AnxA2 downregulation was obtained by Dicer-generated siRNA duplexes (20). Briefly, an amplicon of the target sequence (nucleotides 1-320 from human AnxA2 cDNA, PCR oligos for T7-promoter based cloning: TAA TAC GAC TCA CTA TAA GGG AGA ATG TCT ACT GTT CAC G sense and TAA TAC GAC TCA CTA TAG GGA GAC TGA GCA GGT GTC TTC antisense) was transcribed *in vitro* to generate dsRNA; dicing reaction and d-siRNAs purification were done accordingly to the manufacturer's instructions (Invitrogen). HeLa and BHK cells were transfected 6h after seeding with Fugene-6 (Roche Diagnostics) for cDNA (total time of overexpression: 48h) and with lipofectamine 2000 (Invitrogen), 24h after seeding, for RNAi experiments (total time for silencing: 72h).

In vivo endocytic transport assay - Cells were grown on coverslips and then incubated with 3mg/mL rhodamin-dextran for 10min at 37°C in GMEM containing 10 mM Hepes. Alternatively, cells were re-incubated in marker-free medium for an additional 40min at 37°C. Then, cells were fixed and processed for immunofluorescence, as below.

Microscopy - Cells cultured on coverslips were fixed with 3% PFA and permeabilized with 0.1% saponin in PBS with 10% serum buffer except when using special permeabilization buffer, before fixation, containing 0.1% Triton 100X in 100mM KCl, 2mM $MgCl_2$, 1mM $CaCl_2$ and 1mM Hepes pH 6.9. Pictures were captured with a Zeiss Axiophot microscope, equipped with a 63x Plan-Neofluar objective, or with a Zeiss LSM 510 META confocal microscope equipped with a 63x Plan-Apochromat objective and HeNe1, HeNe2 and Argon lasers. To quantify the colocalization between EEA1 and $AnxA2^{GFP}$ fusions proteins we counted the number of EEA1-positive structures that also contained $AnxA2^{GFP}$ per $100\mu m^2$ in each focal plane. Similarly, the number of vesicles containing Lamp1 and rhodamin-dextran (after pulse-chase internalization as above) after mock-, AnxA2-RNAi with or without AnxA2 cDNAs was quantified by counting the number of vesicles containing both markers per 100 μm^2 in each focal plane.

Subcellular fractionation - Early and late endosomes were purified as previously described (28). The analysis of total membranes and cytosol was carried out by high-speed centrifugation of post-nuclear supernatants (70.000 rpm for 30min). Membranes and cytosol were recovered from the high-speed pellet (HSP) and high-speed supernatant (HSS), respectively.

Biochemical analysis - Total cell lysates were prepared using TNE buffer (20 mM tris pH 7.4, 150 mM NaCl, 1 mM EDTA), and proteases inhibitors (10µM aprotinin, 10µM leupeptin and 1µM pepstatin) and 1% NP40. For immunoprecipitation assays, this lysis buffer was supplemented with 10% glycerol. Briefly, cell extracts or purified endosomes from transfected BHK or HeLa cells were diluted with TNE buffer to a final NP40 concentration of 1%, complemented with 4µg anti-GFP antibody and proteinA-Sepharose beads (Amersham), and incubated for 2h at 4°C. Beads were then washed with TNE buffer with 10% glycerol and resuspended in Laemmli buffer (29). Lysates and immunoprecipitates were analyzed by SDS-PAGE, using 12% acrylamide gels, and western blotting. For p11 western blotting analysis, PVDF (Millipore) membranes were used. Western blotting was carried out using the SuperSignal® West Pico chemiluminescent substrate (Pierce Chemical Co); exposure times were always within the linear range of detection. Chemiluminescent signal was quantified with ImageJ software (NIH).

Annexin A2 binding to liposomes - Five µg of purified recombinant protein (anxA2*wt*, anxA2Y23A, anxA2Y23D) were incubated with liposomes containing phosphatidic acid (PA):phosphatidylethanolamine (PE):cholesterol, (2:2:1) in 50mM Hepes, 1mM EGTA (pH 7.4), 100mM KCl buffer, 5µM DTT, 0.5mM $MgCl_2$, 12.5mM Tris-HCl, 4mg/ml cytosol prepared from BHK cells, phosphatase inhibitors (0.1mM NaF and 10mM orthovanadate) and an ATP-regenerating system for 30min at 4°C (30,31). In some experiments, the mixture was further incubated for 3h at 37°C, as indicated. The binding reaction was stopped by snap freezing in liquid nitrogen. Liposome-bound and free recombinant protein was separated by ultracentrifugation at 35.000 rpm for 60min at 4°C, and analyzed by SDS gels and western blotting with the monoclonal H28 antibody was used against recombinant AnxA2. In immunoprecipitation experiments, liposomes after floatation were mixed with TNE buffer, brought to a final NP40 concentration of 1%, complemented with 2µg anti-AnxA2 antibody H28 and proteinA-Sepharose beads (Amersham), and incubated for 2h at 4°C. Beads were then washed with TNE buffer with 10% glycerol and resuspended in Laemmli buffer (29).

RESULTS AND DISCUSSION

Endosomal AnxA2 is phosphorylated on Tyr23. To investigate the possible role of AnxA2 phosphorylation in endosome association, cells were transfected with AnxA2

tagged with GFP (anxA2*wt*^{GFP}), which shows the same distribution as the endogenous protein (20). After immunoprecipitation from total HeLa cell lysates with anti-GFP antibodies, phosphorylated AnxA2 could be revealed by western blotting with anti-phosphotyrosine, but not anti-phosphoserine, antibodies (Fig 1A). As a control, we mutated the two known N-terminal phosphorylation sites Tyr23 and Ser25 to Ala (double mutant Y23AS25A, anxA2dmt^{GFP}). Although expressed to the same levels as the WT protein, the mutant showed no detectable levels of phosphorylation after immunoprecipitation (Fig 1A). It thus appears that unstimulated cells contain AnxA2 phosphorylated on Tyr23, but perhaps not on Ser25, under steady state conditions.

Using a well-established fractionation protocol (28), early endosome fractions were prepared from BHK cells transfected with anxA2*wt*^{GFP}. The recovery of early endosomes containing the early endosome markers Rab5 and its effector EEA1, but not the late endosome marker Rab7, was not affected by anxA2*wt*^{GFP} expression (Fig 1B). Western blotting with anti-phosphotyrosine and anti-phospho-serine antibodies revealed that a fraction of endosomal anxA2*wt*^{GFP} was phosphorylated on Tyr (figure 1C, right panel) but apparently not on serine (not shown).

Efficient endosome targeting depends on AnxA2 phosphorylation. Next, we investigated whether phosphorylation plays a role in the regulation of endosomal membrane binding, and analyzed the subcellular distribution of WT and mutant protein by confocal microscopy. The WT protein was present in the cytosol and colocalized with EEA1 on early endosomes (Fig 2A, arrowheads), as expected (19 ,20,28). By contrast, the mutant protein was predominantly cytosolic and showed little colocalization with EEA1 (Fig 2A arrowheads — the yellow color in the merge reflects the overlap between cytosolic anxA2dmt^{GFP} and EEA1 punctae), as illustrated by the quantification of WT and mutant AnxA2 co-localization with EEA1 (figure 2B).

After homogenization and high speed centrifugation, anxA2*wt*^{GFP} was enriched approximately 2 fold in membranes when compared to the cytosol fraction, like endogenous anxA2 (Fig 2C, quantification in the inset), as expected (23). By contrast, anxA2dmt^{GFP} showed the opposite distribution, being enriched approximately 2 fold in cytosol (Fig 2C, quantification in the inset), in good agreement with our microscopy analysis (figure 2A). Finally, after endosome preparation by subcellular fractionation, both anxA2*wt*^{GFP} and anxA2dmt^{GFP} copurified with endogenous AnxA2 and the transferrin receptor and to a lesser extent with Rab7 — anxA2*wt*^{GFP} was somewhat more abundant in late endosomes after overexpression (Fig 2D). Strikingly, however, early endosomes contained roughly half as much anxA2dmt^{GFP} when compared to anxA2*wt*^{GFP} (Fig 2D, quantification in inset), although the two proteins were expressed to similar levels (Fig 2D). Altogether these observations show that membrane association of AnxA2 is impaired after mutagenesis of its phosphorylation sites.

Annexin A2 tyrosine phosphorylation is required for endosomal association. To identify which phosphorylation site, Tyr23 or Ser25, was necessary for endosome membrane association, we constructed two AnxA2 single-point mutants, anxA2Y$_{23}$A^{GFP} and anxA2S$_{25}$A^{GFP}, in which Tyr23 or Ser25 had been mutated. Equal amounts of anxA2*wt*^{GFP}, anxA2Y$_{23}$A^{GFP} and anxA2S$_{25}$A^{GFP} could be detected in total cell lysates (Fig 3A). Yet, after high speed centrifugation, anxA2S$_{25}$A^{GFP} shown the same distribution as the WT protein being more abundant than anxA2Y$_{23}$A^{GFP} (Fig 3B). Similarly, after subcellular fractionation, anxA2S$_{25}$A^{GFP} and the WT protein were equally abundant on endosomes (Fig 3A). By contrast, anxA2Y$_{23}$A^{GFP} was significantly reduced (Fig 3A) and showed the same distribution as the double phosphorylation mutant (Fig 2D).

To further investigate the role of Tyr23 phosphorylation, we generated a phospho-mimicking mutant by replacing the tyrosine residue with an aspartic acid (anxA2Y$_{23}$D^{GFP}). When analyzed by light microscopy, the two tyrosine mutants of anxA2 (AnxA2Y$_{23}$A^{GFP} and anxA2Y$_{23}$D^{GFP}) showed very different behavior. anxA2Y$_{23}$A^{GFP} was predominantly cytosolic (Fig 4A, quantification in Fig 4B), like the double mutant (Fig 2A). By contrast, anxA2Y$_{23}$D^{GFP} showed essentially the same

distribution as the WT protein. This mutant colocalized extensively with EEA1 on early endosomes, perhaps even more so that the WT protein (Fig 4A, quantification in Fig 4B). Similarly, anxA2$Y_{23}D^{GFP}$, but not anxA2$Y_{23}A^{GFP}$, showed the same distribution as the WT protein after fractionation (Fig 4C). Altogether, these observations demonstrate that endosome membrane association depends on Tyr23 phosphorylation of AnxA2.

Annexin A2 binding to liposomes. AnxA2 exhibits the intrinsic capacity to bind negatively charge phospholipids via its C-terminal core domain, presumably in a calcium-dependent manner (2), and association to the endosomes depends on membrane cholesterol (19). Consistently, the purified recombinant form of AnxA2*wt* (Fig 5A) was able to bind efficiently liposomes containing phosphatidic acid (PA), phophatidyl-ethanolamine (PE) and cholesterol after incubation for 30min at 4°C (19) (not shown). AnxA2*wt* also bound liposomes in the presence of cytosol, ATP and phosphatase inhibitors (Fig 5B) with the same efficiency as without cytosol (not shown). In these experiments, we used the H28 monoclonal antibody that recognizes the AnxA2 fusion proteins but not endogenous AnxA2 (20,32,33). Similarly, AnxA2$Y_{23}A$ and AnxA2$Y_{23}D$ (Fig 5A), which both contain an intact C-terminus, showed the same liposome binding capacity as the WT protein in the presence (Fig 5B, quantification in Fig 5C) or absence (not shown) of cytosol, ATP and phosphatase inhibitors at 4°C.

AnxA2*wt* was then incubated with liposomes in the presence of cytosol, ATP and and phosphatase inhibitors for 3h at 37°C. Liposomes were retrieved by floatation and AnxA2 was immuno-precipitated from the liposome fraction with the H28 anti-AnxA2 antibody, which only recognizes the recombinant protein. Immunoblotting of the precipitate with antibodies against phospho-tyrosine showed that recombinant AnxA2*wt* bound to liposomes had been efficiently phosphorylated during the in vitro incubation (Fig 5D). Under these conditions, AnxA2*wt* was indeed detected on the liposomes (Fig 5B, lower panel) and binding occurred with an efficiency similar to that observed at 4°C (Fig 5C). It is not easy to compare directly the absolute amounts of AnxA2*wt* bound at 4°C and 37°C, since the protein interacts with lipids and since bilayer fluidity is different at these temperatures. However, these experiments unambiguously show that AnxA2 is phosphorylated when bound to liposomes.

Strikingly, liposome association of AnxA2$Y_{23}A$ and AnxA2$Y_{23}D$ were significantly decreased and increased, respectively (Fig 5B, quantification in Fig 5C) after 3h at 37°C. This may reflect differences in the capacity of each mutant to interact with putative cytosolic partners. However, both mutants interacted with the AnxA2 light chain p11 with the same efficiency as the WT protein (Fig S1), indicating that p11 is unlikely to regulate membrane association, in accordance with our previous findings (20). We also found that actin, another well-established AnxA2 partner, interacted preferentially with AnxA2$Y_{23}D$ when compared to AnxA2$Y_{23}A$ or to the wt protein (Fig S2), suggesting that Tyr23 phosphorylation regulates interactions with actin. Conversely, however, AnxA2 membrane association is unlikely to be controlled by interactions with actin, since actin depolymerization with latrunculin B did not affect AnxA2 binding to endosomes (Fig S2). Thus, the simplest interpretation of our observations is that, the $Y_{23}D$ mutation, and presumably Tyr23 phosphorylation, increases membrane association at 37°C, when membrane fluidity is high, by causing a conformational change that stabilizes the protein onto the membrane. Consistently, we observed that liposome binding of AnxA2$Y_{23}D$ compared to AnxA2$Y_{23}A$ is increased, when the incubation was at 37°C without cytosol (Fig 5E).

Annexin A2 endosomal function requires tyrosine phosphorylation. We previously showed that AnxA2 depletion by RNA interference inhibits membrane transport beyond early endosomes along the pathway leading to lysosomes (19 ,20). To this end, we monitored early-to-late endosome transport using rhodamin-dextran internalized for 5min at 37°C and then chased for 40min in marker-free medium. In control cells, the tracer reached Lamp1-positive late endocytic compartments, as expected, (Fig 6A; quantification in Fig 6C). After AnxA2 knockdown with Dicer-generated siRNAs (Fig

6B), as in our previous studies (20), rhodamin-dextran internalization was not affected (not shown), as expected (19,20). However, as in our previous studies (19,20) little tracer reached Lamp1-positive late endosomes and intracellular levels were significantly decreased (Fig 6A, quantification in Fig 6C) — most likely, the tracer had then been recycled to the medium, rather than transported to late endosomes and lysosomes.

Next we investigated whether early-to-late endosome transport could be restored by ectopic expression of the WT protein after AnxA2 depletion. After AnxA2 knockdown with siRNAs, anxA2*wt*^{GFP}, anxA2Y$_{23}$A^{GFP} or anxA2Y$_{23}$D^{GFP} could be efficiently re-expressed and expression levels were similar (Fig 6B). RNAi resistance was presumably due to the use of a modified human AnxA2 cDNA (nucleotide 197, (20,32,33)) that also contains a silent mutation in nucleotide 345 — the target sequence of our siRNA covers ≈350 first base pairs of human AnxA2 mRNA. Moreover, the two phosphorylation mutants bear mutations in nucleotide 70 (corresponding to Tyr23). Re-expression of the WT protein restored early-to-late endosome transport, unambiguously demonstrating that the inhibition of endocytic transport observed after AnxA2 depletion was not due to some off-target effect (Fig 6A, quantification in Fig 6C). Strikingly, early-to-late endosome transport could be rescued by re-expression of the phospho-mimicking mutant anxA2Y$_{23}$D^{GFP}, but not of anxA2Y$_{23}$A^{GFP} (Fig 6A, quantification in Fig 6C). This observations show that Tyr23 is essential for AnxA2 functions in endocytic membrane traffic, presumably because its phosphorylation regulates association to endosome membranes.

CONCLUSION

Endosomal AnxA2 is known to regulate endocytic membrane traffic, and in particular membrane transport from early to late endosomes (18-20,22), The protein shows a non-random distribution on endosomes, and is associated to membranes via an unconventional lipid-dependent mechanism (19,23), which requires the intact AnxA2 N-terminus (2). The hypervariable N-terminal domain of AnxA2 contains the Tyr23 and Ser25 phosphorylation sites as well as the binding site for p11/S100A10, the AnxA2 ligand (2). While we previously found that p11/S100A10 is not involved in AnxA2 endosomal functions (20), we now show that Tyr23 phosphorylation controls AnxA2 binding to endosomal membranes, and thus its functions in transport — highlighting the role of the N-terminus, as recently suggested by in vitro approach with artificial membranes (34).

Our experiments indicate that Tyr23 phosphorylation regulates positively the binding of monomeric AnxA2 to endosomes. However, non-phosphorylated AnxA2 is also expected to be present on endosomes. In fact, our data argue that non-phosphorylable AnxA2 can bind endosomes, but may be less efficiently retained onto the membrane. Phosphorylation may thus help stabilize AnxA2 onto the membrane, rather than acting as an "on-off" switch. It is tempting to propose that monomeric AnxA2 binds endosomes independently of Tyr23 phosphorylation, via phospholipids and cholesterol (2,19,22): phosphorylation may then stabilize membrane-associated protein, perhaps via a conformational change that may help dipping of the amphipatic N-terminal helix into the bilayer, and/or facilitate oligomerization of AnxA2.

In conclusion we show here that both binding and transport-related functions of endosomal AnxA2 are positively regulated by tyrosine phosphorylation in the N-Terminal part of the protein, highlighting the fact that AnxA2 functions are differentially regulated by specific signaling mechanisms on the different subcellular sites.

REFERENCES

1. Futter, C. E., and White, I. J. (2007) *Traffic*
2. Gerke, V., and Moss, S. E. (2002) *Physiol Rev* **82**, 331-371
3. Rescher, U., and Gerke, V. (2004) *J Cell Sci* **117**, 2631-2639

4. Rety, S., Sopkova, J., Renouard, M., Osterloh, D., Gerke, V., Tabaries, S., Russo-Marie, F., and Lewit-Bentley, A. (1999) *Nat Struct Biol* **6**, 89-95
5. Gerke, V., and Weber, K. (1984) *Embo J* **3**, 227-233
6. Glenney, J. R., Jr. (1985) *FEBS Lett* **192**, 79-82
7. Gould, K. L., Woodgett, J. R., Isacke, C. M., and Hunter, T. (1986) *Mol Cell Biol* **6**, 2738-2744
8. Johnstone, S. A., Hubaishy, I., and Waisman, D. M. (1992) *J Biol Chem* **267**, 25976-25981
9. Regnouf, F., Sagot, I., Delouche, B., Devilliers, G., Cartaud, J., Henry, J. P., and Pradel, L. A. (1995) *J Biol Chem* **270**, 27143-27150
10. Deora, A. B., Kreitzer, G., Jacovina, A. T., and Hajjar, K. A. (2004) *J Biol Chem* **279**, 43411-43418
11. He, K. L., Deora, A. B., Xiong, H., Ling, Q., Weksler, B. B., Niesvizky, R., and Hajjar, K. A. (2008) *J Biol Chem*
12. Hubaishy, I., Jones, P. G., Bjorge, J., Bellagamba, C., Fitzpatrick, S., Fujita, D. J., and Waisman, D. M. (1995) *Biochemistry* **34**, 14527-14534
13. Bellagamba, C., Hubaishy, I., Bjorge, J. D., Fitzpatrick, S. L., Fujita, D. J., and Waisman, D. M. (1997) *J Biol Chem* **272**, 3195-3199
14. Rescher, U., Ludwig, C., Konietzko, V., Kharitonenkov, A., and Gerke, V. (2008) *J Cell Sci* **121**, 2177-2185
15. de Graauw, M., Tijdens, I., Smeets, M. B., Hensbergen, P. J., Deelder, A. M., and van de Water, B. (2008) *Mol Cell Biol* **28**, 1029-1040
16. Matsuda, D., Nakayama, Y., Horimoto, S., Kuga, T., Ikeda, K., Kasahara, K., and Yamaguchi, N. (2006) *Exp Cell Res* **312**, 1205-1217
17. Emans, N., Gorvel, J. P., Walter, C., Gerke, V., Kellner, R., Griffiths, G., and Gruenberg, J. (1993) *J Cell Biol* **120**, 1357-1369
18. Zobiack, N., Rescher, U., Ludwig, C., Zeuschner, D., and Gerke, V. (2003) *Mol Biol Cell* **14**, 4896-4908
19. Mayran, N., Parton, R. G., and Gruenberg, J. (2003) *Embo J* **22**, 3242-3253
20. Morel, E., and Gruenberg, J. (2007) *PLoS ONE* **2**, e1118
21. Jost, M., Zeuschner, D., Seemann, J., Weber, K., and Gerke, V. (1997) *J Cell Sci* **110 (Pt 2)**, 221-228
22. Gruenberg, J., and Stenmark, H. (2004) *Nat Rev Mol Cell Biol* **5**, 317-323
23. Harder, T., Kellner, R., Parton, R. G., and Gruenberg, J. (1997) *Mol Biol Cell* **8**, 533-545
24. Rescher, U., Zobiack, N., and Gerke, V. (2000) *J Cell Sci* **113 (Pt 22)**, 3931-3938
25. Petiot, A., Faure, J., Stenmark, H., and Gruenberg, J. (2003) *J Cell Biol* **162**, 971-979
26. Kobayashi, T., Beuchat, M. H., Lindsay, M., Frias, S., Palmiter, R. D., Sakuraba, H., Parton, R. G., and Gruenberg, J. (1999) *Nat Cell Biol* **1**, 113-118
27. Kobayashi, T., Stang, E., Fang, K. S., de Moerloose, P., Parton, R. G., and Gruenberg, J. (1998) *Nature* **392**, 193-197
28. Aniento, F., Emans, N., Griffiths, G., and Gruenberg, J. (1993) *J Cell Biol* **123**, 1373-1387
29. Laemmli, U. K. (1970) *Nature* **227**, 680-685
30. Gruenberg, J., Griffiths, G., and Howell, K. E. (1989) *J Cell Biol* **108**, 1301-1316
31. Tuomikoski, T., Felix, M. A., Doree, M., and Gruenberg, J. (1989) *Nature* **342**, 942-945
32. Johnsson, N., Johnsson, K., and Weber, K. (1988) *FEBS Lett* **236**, 201-204
33. Thiel, C., Weber, K., and Gerke, V. (1991) *FEBS Lett* **285**, 59-62

34. Zibouche, M., Vincent, M., Illien, F., Gallay, J., and Ayala-Sanmartin, J. (2008) *J Biol Chem*

FOOTNOTE

*We are grateful to Marie-Claire Velluz for technical assistance and to Zeina Chamoun for AnxA2 siRNA duplexes and for comments on the manuscript. We warmly thank Monique Rousset for comments on the manuscript and Völker Gerke for AnxA2 and AnxA2-GFP cDNA. Support was from the Swiss National Science Foundation, the Telethon Foundation (both to J.G.), as well as the Fondation pour la Recherche Medicale (FRM) and the Roche Research Foundation (to E.M.).

FIGURES LEGENDS

Fig. 1. endosomal AnxA2 is phosphorylated on tyrosine 23. (A), HeLa cells were transfected with anxA2*wt*^{GFP} or with anxA2*dmt*^{GFP}, in which both Tyr23 and Ser25 were mutated to Ala. Cells were homogenized and the GFP fusion proteins were immunoprecipitated from the lysates with anti-GFP antibodies (IP Ab^{+}: immunoprecipitate; IP Ab^{-} : control without the specific antibody; load: input fraction before immunoprecipitation). Immunoprepipitates and one tenth of the load volumes were analyzed by SDS-PAGE and western blotting with the indicated antibodies: anti-GFP antibody (upper panels), anti-phosphoserine (middle panels) and anti-phosphotyrosine (lower panels). IgG HC, heavy chain of anti-GFP antibody used for immunoprecipitation. (B), BHK cells were (anxA2*wt*^{GFP}) or not (NT) transfected with anxA2*wt*^{GFP}. Early endosomes were prepared using a well-established fractionation protocol (28), and analyzed by SDS-PAGE and western blotting. The fractions contain the early endosomal markers EEA1 and Rab5, but not the late endosomal marker Rab7. (C), anxA2*wt*^{GFP} was immunoprecipitated with anti-GFP antibodies from early endosomal fractions prepared as in (B). Ab+: immunoprecipitate; Ab^{-}: control without the specific antibody; EE load: input fraction before immunoprecipitation (early endosomes). Immunoprepipitates and half of the load volumes analyzed by SDS-PAGE and western blotting with the indicated antibodies. IgG HC, heavy chain of anti-GFP antibody used for immunoprecipitation.

Fig. 2. AnxA2 phosphorylation mutants and early endosomes localization. (A), HeLa cells were transfected with anxA2*wt*^{GFP} (left panel) and anxA2*dmt*^{GFP} (right panels), labeled with–antibodies against EEA1 and analyzed by double channel fluorescence microscopy. Arrows point at examples of GFP-fusion protein colocalization with EEA1. Bar 10 µm. (B), the number of GFP-labeled structures that also contained EEA1 was counted and is expressed as a percentage of anxA2*wt*^{GFP}. n=5. (C), BHK cells were transfected with anxA2*wt*^{GFP} or anxA2*dmt*^{GFP}, and homogenized. The lysate was fractionated by high speed centrifugation, and pellets (membranes, memb) and supernatants (cytosol) were analyzed by SDS-PAGE (equal protein amounts loaded in each lane) and blotted using anti-GFP antibody (upper panels) and anti-AnxA2 HH7 antibody (lower panel). The blots were scanned and the inset shows the fold enrichment in membranes over the cytosol. n=5. (D) BHK cells were transfected with anxA2*wt*^{GFP} or anxA2*dmt*^{GFP}. Early (EE) and late (LE) endosomes were prepared using the same fractionation protocol as in Fig 1B-C and analyzed by SDS-PAGE and western blotting using the indicated antibodies (equal protein amounts loaded in each lane). The early endosome blots were scanned and the amounts of anxA2dmt^{GFP} present in early endosomes are expressed as a percentage of the anxA2*wt*^{GFP} control. n=8.

Fig. 3. Association of tyrosine 23 and serine 25 mutants to membranes. (A), BHK cells were transfected with anxA2*wt*^{GFP}, anxA2Y$_{23}$A^{GFP} or anxA2S$_{25}$A^{GFP}. Cell lysates (upper panels) and early endosomes (EE, lower panels) were prepared and analyzed by SDS gels (equal protein amounts loaded in each lane) and blotted with anti-GFP and anti-rab5 antibodies. (B), Cells were transfected as in (A) and membranes (memb) and cytosol prepared as in Fig 2C were analyzed by SDS-PAGE (equal protein amounts loaded in each lane) and blotted using anti-GFP antibody and anti-Rab5 antibody.

Fig. 4. Distribution of AnxA2 single tyrosine mutant. (A), HeLa cells were transfected with anxA2*wt*^{GFP}, anxA2Y$_{23}$A^{GFP} or anxA2Y$_{23}$D^{GFP} and analyzed by immunofluorescence using antibodies against EEA1. Bar 10 µm, arrowheads point at examples of GFP colocalization with EEA1. (B) As in Fig 2B, the number of GFP-labeled structures that also contained EEA1 was counted and is expressed as a percentage of anxA2*wt*^{GFP}. n=3. (C), Early endosomes were prepared from BHK cells transfected with anxA2*wt*^{GFP}, anxA2Y$_{23}$A^{GFP} or anxA2Y$_{23}$D^{GFP}, analyzed by SDS-PAGE (equal protein amounts loaded in each lane) and blotted with anti-GFP antibody (upper panel) and antibodies against annexin A2, and rab5 (lower panels).

Fig. 5. Binding to liposomes. (A) AnxA2wt, anxA2Y$_{23}$A or anxA2Y$_{23}$D were expressed in bacteria, purified and analyzed in SDS gels. The gels were stained with Coomassie blue. (B) PA/PE/cholesterol liposomes were prepared and incubated in vitro with 5µg purified recombinant anxA2wt, anxA2Y$_{23}$A or anxA2Y$_{23}$D, for 30min at 4°C in the presence of cytosol, ATP-regenerating system and phosphatase inhibitors (upper panel) or further incubated for 3h at 37°C (lower panel) in the same mixture, as indicated. Liposomes were then recovered by floatation in sucrose gradients and separated from the load containing free protein. Liposome-bound (bound) and free AnxA2 were analyzed by SDS-PAGE and western blotting using H28 monoclonal antibody that recognizes the recombinant proteins. (C), the blots in (B) were scanned and the amounts of recombinant protein associated to liposomes are expressed as a percentage of the AnxA2wt. n=3. (D) PA/PE/cholesterol liposomes were prepared and incubated in vitro with 5µg purified recombinant anxA2wt for 30min at 4°C in the presence of cytosol, ATP-regenerating system and phosphatase inhibitors and then for 3h at 37°C, as in B. Liposomes were then recovered by floatation in sucrose gradients and recombinant anxA2 was immunoprecipitated from the liposome fraction with H28 anti-annexin A2 antibody. The immunoprecipitate and the initial reaction mixture (react mix) were analyzed by SDS-PAGE and western blotting using the H28 monoclonal antibody (right panel) and anti-phosphorylated tyrosine antibody (P-tyr, left panel). The position of AnxA2 is indicated with an arrow. The heavy chain of IgG used in immunoprecipitation is also indicated (IgG HC). (E) PA/PE/cholesterol liposomes were incubated in vitro with 5µg purified recombinant AnxA2Y$_{23}$A or AnxA2Y$_{23}$D for 3h at 37°C as in (B), but without cytosol, ATP regenerating system or phosphatase inhibitors. The panel shows a representative experiment analyzed as in (B).

Fig. 6. Re-expression of AnxA2 mutants after knockdown. (A-B), AnxA2 was (siRNA) or not (control, ctrl) knocked down in HeLa cells with diced siRNAs (20). Then, cells were or not transfected with anxA2*wt*^{GFP}, anxA2Y$_{23}$A^{GFP} or anxA2Y$_{23}$D^{GFP} cDNAs, as indicated. Cells were either homogenized and analyzed by SDS-page and western blotting with the indicated antibodies (B) or incubated with rhodamine-dextran (red channel) for 10min at 37°C followed by a 40min chase without the marker (A). Then, cells were fixed and labeled with antibodies against lamp1 (blue channel). Bar: 10µm. (C). The number of endosomes containing dextran and Lamp1 was counted and is expressed ad a percentage of the total number in the untreated control. n=4.

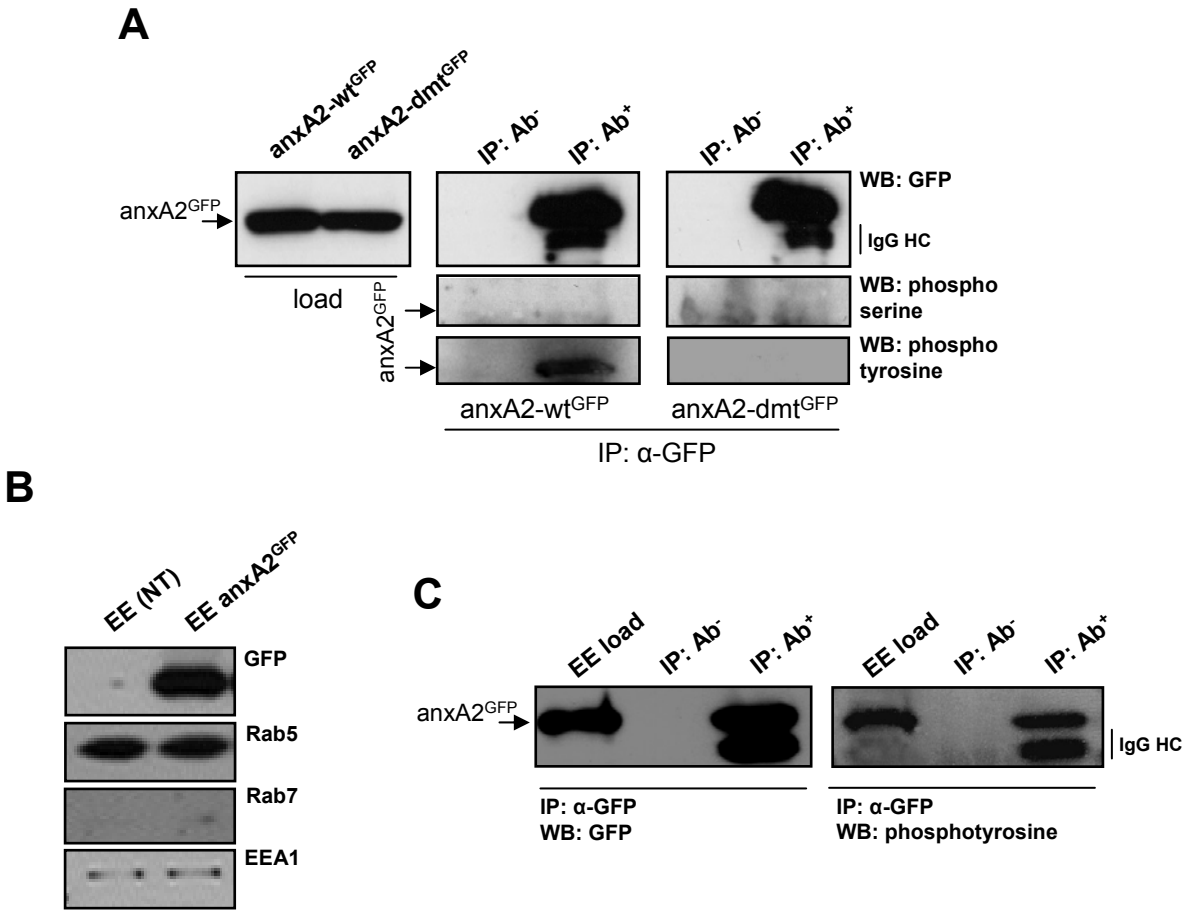

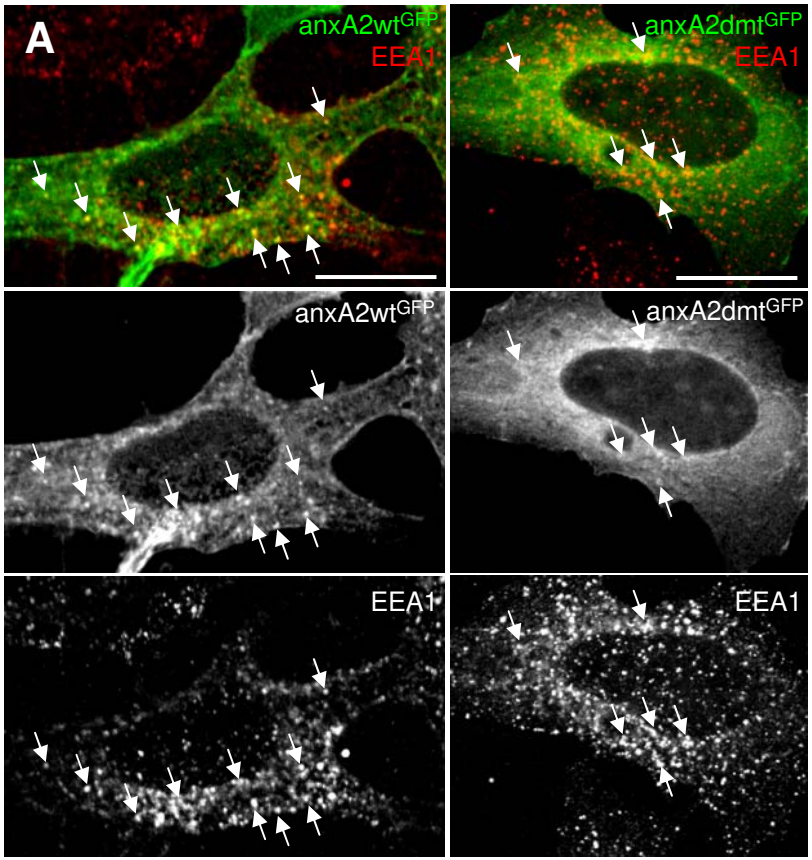

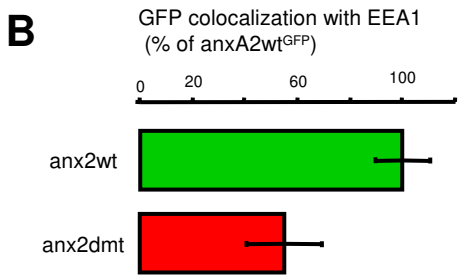

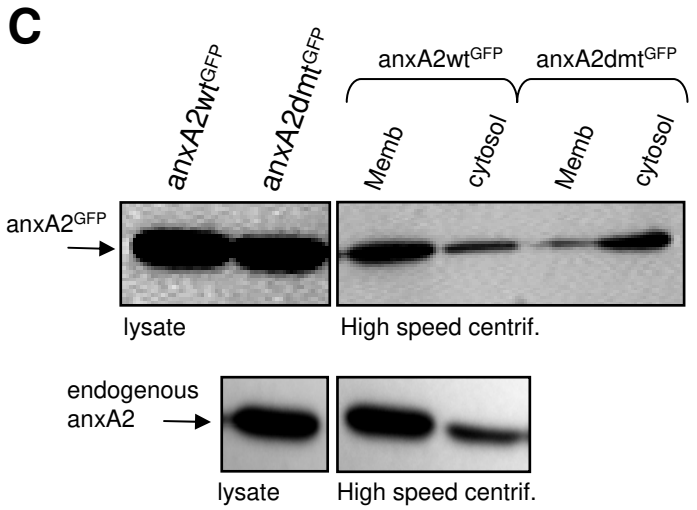

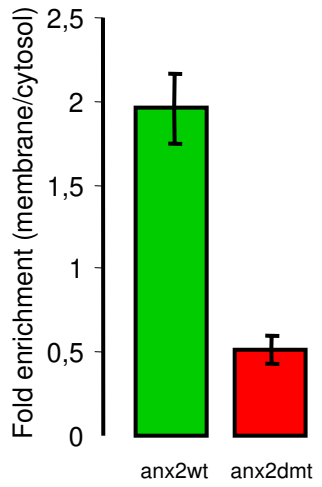

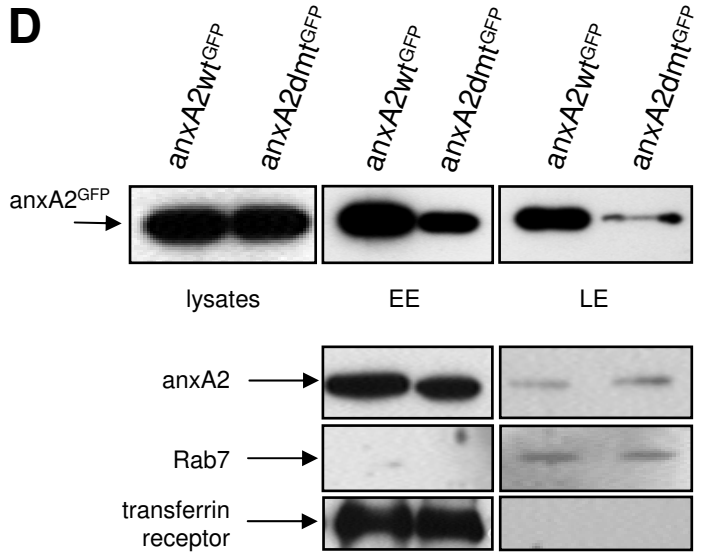

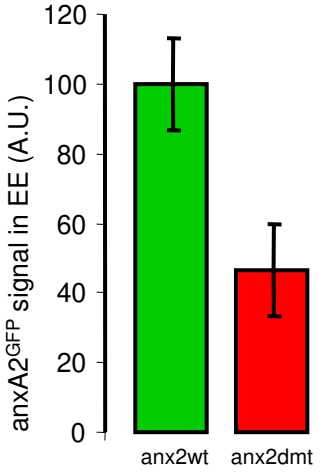

Morel Figure 3

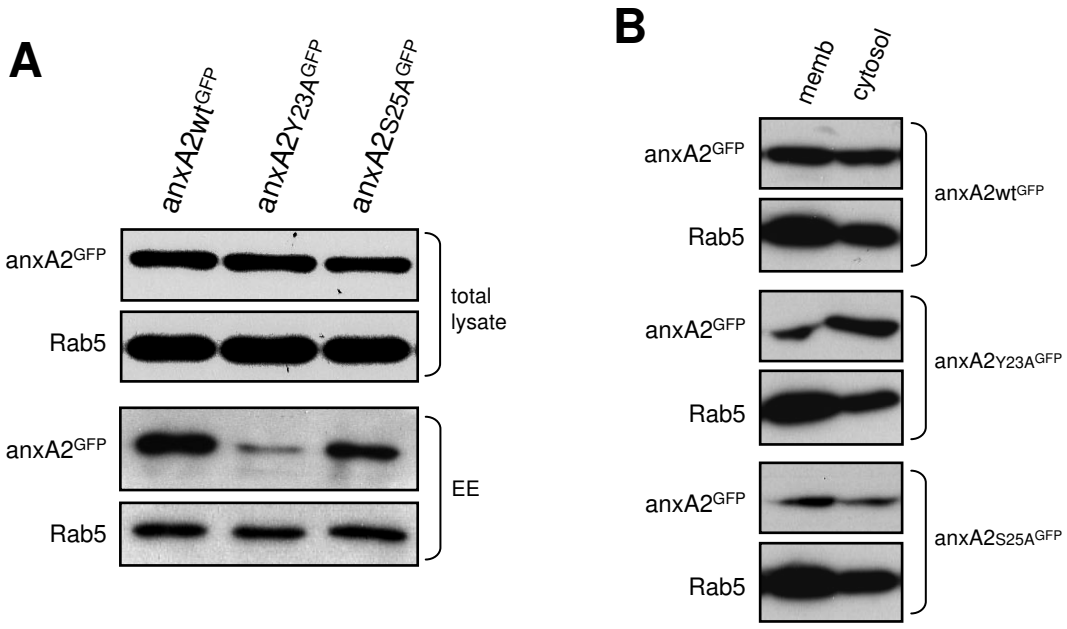

Morel Figure 4

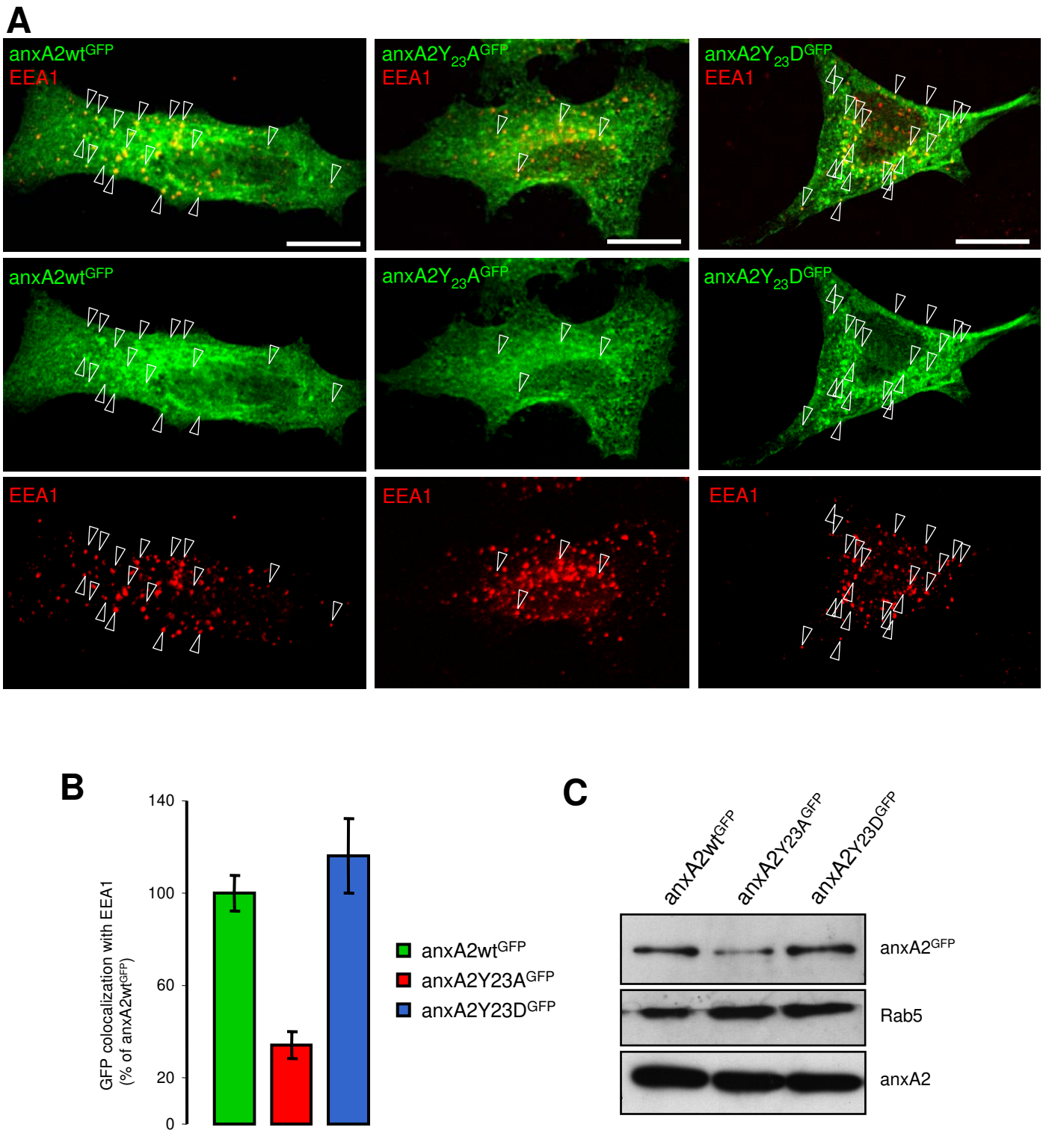

Morel Figure 5